

Optimal Dolphin-style soaring

E.D. Dickmanns

Presented at the XVII OSTIV Congress, Paderborn, Germany (1981)

Abstract

A set of optimal trajectories is given for straight flights through vertical windfields of different extensions with one glider (LS3, 15-m class). Two types of optimal trajectories exist which in some regions appear in parallel as local optima. The phuboid wavelength at the Nickel/MacCready speed is shown to be the deciding factor for the determination of the global optimum. These theoretically optimal trajectories will be hard to pilot for short windfields. For relatively long ones the optimal flight takes place at n_z close to one.

Introduction: In competition soaring maximum range and given range in minimum time are of major interest today. The latter task requires - besides selecting the best route with regard to thermals - also a decision how to use the upwind fields in an optimal fashion: cycling or traversing and if traversing, with which speed and load factor program. Flying from one thermal to the next, the most favourable speed depends on the net climb rate w_N expected in the next thermal and is constant, if there are no vertical winds in between. Nickel [1] and MacCready [2] developed a theory and an instrument to guide the pilot in a simple fashion. If there are upwinds en route simple physical reasoning indicates to slow down in upwinds and to speed up in downwinds in order to improve the performance. But exactly how large these deviations should be is a much more difficult question.

Pierson and de Jong [3] formulated the task as an optimal-control problem and de Jong [4] gave some isolated numerical solutions showing that two different types of optimal trajectories exist.

This paper documents the results obtained by applying the calculus of variations and an algorithm for solving the arising boundary value problem. The mathematical formulation will be given in a forthcoming publication [5] and is

omitted here. The windfield model is an exponential one according to [4] with downwinds surrounding the upwind center (see fig. 2a and c, fig. 4e, dashed curves).

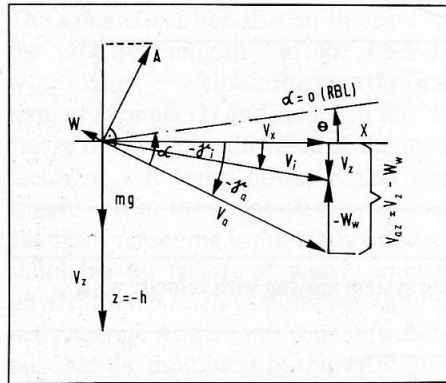


Fig. 1 Axis system and variables used.

Discussion of results: Figure 1 shows the nomenclature with V_x = horizontal and V_z = vertical speed component (positive downward), w_w = upwind (neg.), all given in meters per second [m/s]. $A(C_A)$ is the lift force (coefficient) $A = 0.5 \rho V_a^2 S C_A$ which divided by mass and Earth gravity mg yields the normal load factor n_z , a critical guidance quantity. The performance index Φ is flight time to the starting altitude in the next thermal

$$\Phi = T + \frac{h_0 - h_f}{w_N}$$

where T is cross-country flight time and the second term is the time in the thermal to climb back to h_0 , the initial altitude.

Figure 2 shows range histories of variables for two optimal trajectories, one with a wavelength Δ_A of the windfield of

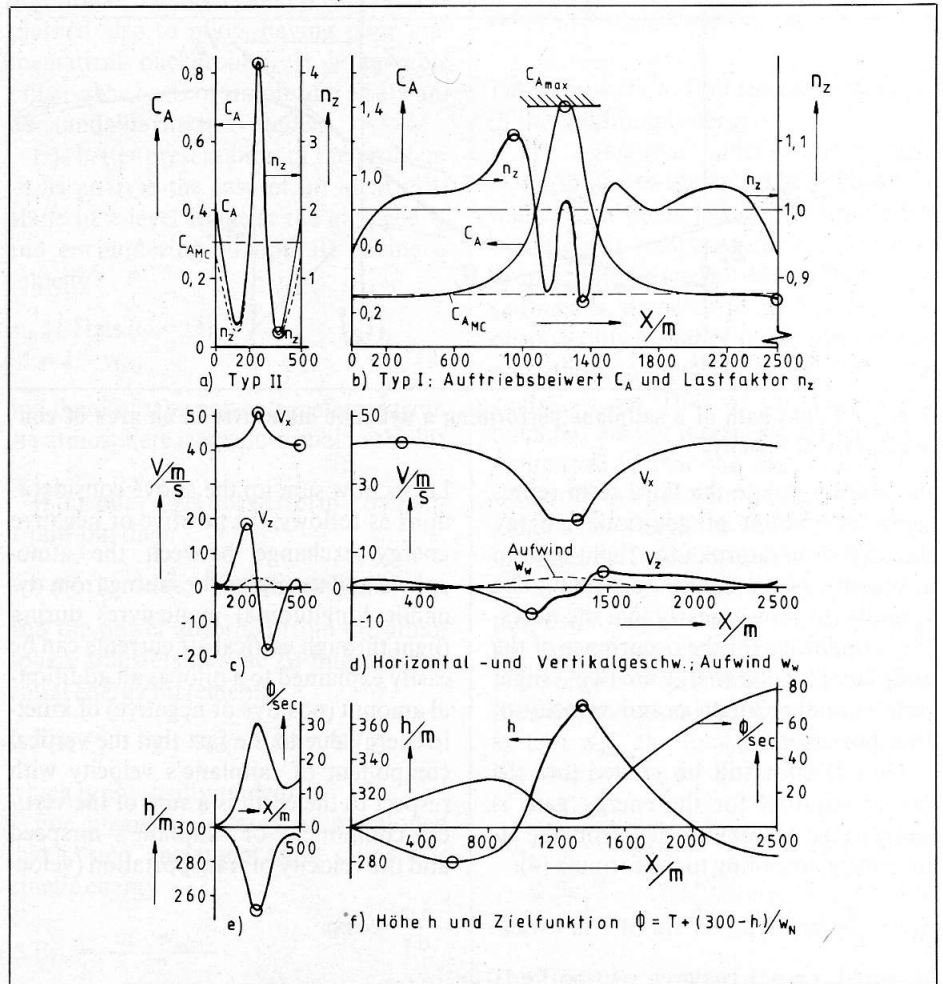


Fig. 2 Optimal trajectories for windfield wavelengths $\Delta_A = 280$ m ($x_f = 500$ m) and 1400 m ($x_f = 2500$ m) for LS-3, wing loading 33 kg/m^2 , $w_N = 2 \text{ m/s}$; $|w_{w\max}| = 3 \text{ m/s}$.

280 m (left, a, c, e), corresponding to $x_f = 500$ m, and the other with a fivefold Δ_A of 1400 m ($x_f = 2500$ m, right). For the latter case the load factor is always close to 1 (.86 to 1.1), see upper right, fig. b), while in the former one it reaches a peak of 4 and two minima ($n_z \approx 0.2$) in the downwind region. The lift coefficient C_A in both cases has a pronounced maximum at the upwind center while the forward speed V_x has a maximum for the short and a minimum for the long wavelength (upper part figures c and d). In order to pick up the speed needed in short windfields for maximum energy transfer at the upwind center by using high g loads (n_z), the glider has to be dashed into the windfield, trading altitude for speed (fig. 2e, lower left). In long wind-

fields the lower speed V_x is achieved by trading kinetic energy for altitude and the climb rate is accentuated by the upwind. When leaving the windfield the situation is reversed. The payoff quantity Φ at the center of the windfield has a relative maximum for the short and minimum for the long wavelength (fig. e and f). The trajectory for large Δ_A is said to be of type I (conventional dolphin-style flight with $n_z \approx 1$), while the one for small Δ_A is termed to be of type II (high g loads).

The extremal values of a trajectory, marked by circles in fig. 2, can be used to characterize this trajectory. Figure 2 shows the family of optimal trajectories existing between the two windfield wavelengths shown in fig. 2. The maximum

upwind is 3 m/s and the net climb rate in the next thermal is assumed to be $w_N = 2$ m/s for a wing loading of 33 kg/m². The flight always starts 0.884 wavelengths before the upwind center and ends the same distance behind it with boundary values according to the Nickel/MacCready speed $V_{XR} = 41.63$ m/s, $V_{ZR} = 1.344$ m/s, h_0 is 300 m. For a new range parameter the initial values needed to start the numerical iteration (required for solving the boundary value problem) were taken from the last converged solution. Surprisingly enough, in a certain region the converged solution depended on the direction of the wavelength parameter change (overlapping dashed curves in figure 3).

Type-I solutions are seen to exist from

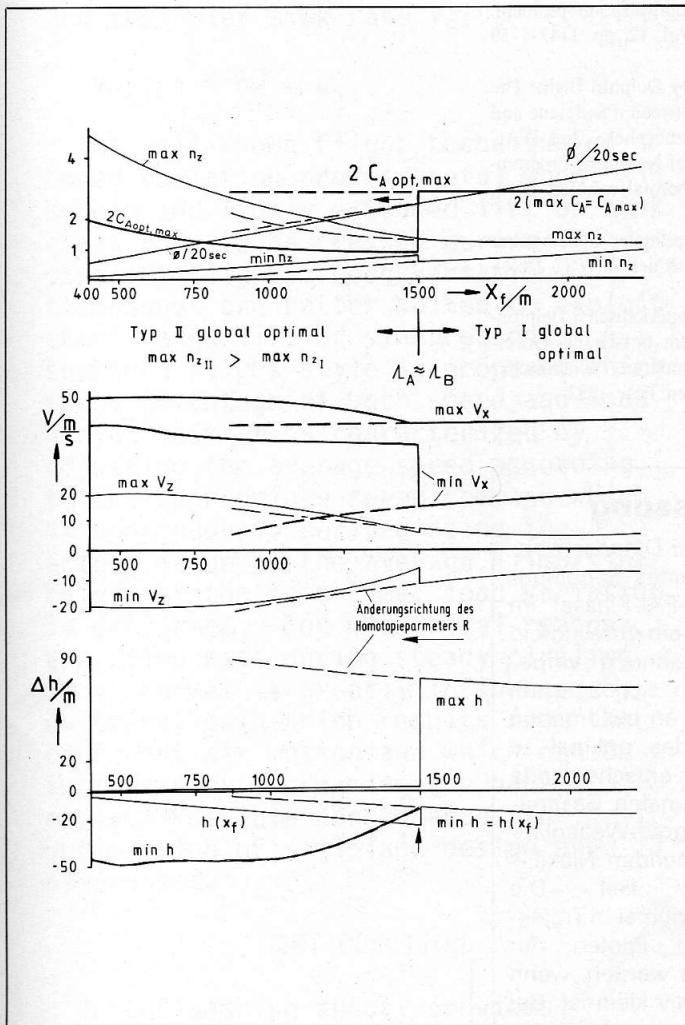


Fig. 3 Extreme values of some variables for a family of solutions between the cases of figure 2.

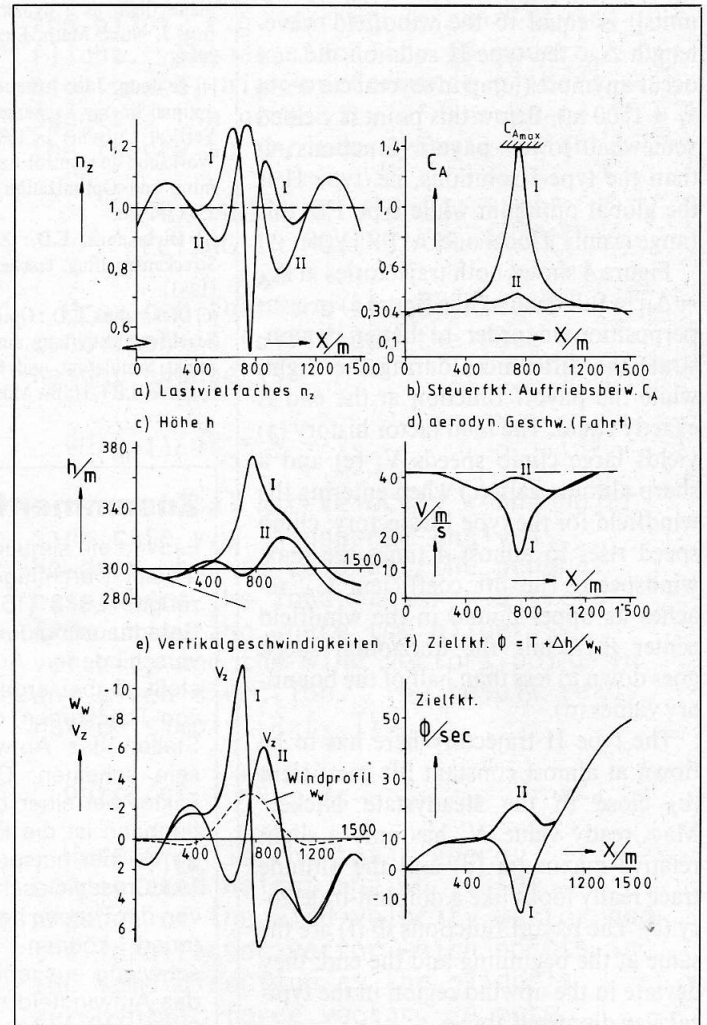


Fig. 4 Two equivalent trajectories with different control histories for the case $\Delta_A = \Delta_B$ ($x_f = 1500$ m, see fig. 3): I trades speed for height, II trades height for speed.

the upper end down to $x_f = 875$ m ($\Delta_A = 310$ m), quickly recognizable by large values of max. lift coefficient $C_{A \text{ opt max}}$ (upper part) and max. altitude h (lower part) as well as by the low value of $V_{x \text{ min}}$ (middle, right). The upper and lower bounds for the loadfactor (max n_z and min n_z , lower curves in upper figure right) both tend towards 1 for increasing windfield lengths.

The type-II solutions (left part of the figure) are marked by high g loads, decreasing with increasing windfield lengths, relatively high values for both max. and min. horizontal speed V_x and by low values of the minimum altitude min h (lower curve).

Beyond a certain range, corresponding to the point where the phugoid wavelength Δ_B at the Nickel/MacCready velocity V_{NM} ($\Delta_B = 0.453 V_{NM}^2$ [metric units]) is equal to the windfield wavelength Δ_A , the type-II solution did not occur anymore (jump in several curves at $x_f = 1500$ m). Below this point it yielded somewhat lower payoff functions Φ than the type-I solutions, i.e. type II is the global optimum while type I in this range is only a local one.

Figure 4 shows both trajectories at $\Delta_A = \Delta_B$ in full details (like figure 2) in a superposition in order to better demonstrate the differences during the flight, while the payoff function at the end is exactly equal. The load factor history (a) yields large climb speeds V_z (e) and a sharp altitude gain (c) when entering the windfield for the type I trajectory; climb speed rises to almost 4 times the max. windspeed. The lift coefficient C_A reaches its upper bound in the windfield center (b) while the horizontal speed goes down to less than half of the boundary values (d).

The type II trajectory here has to be flown at almost constant lift coefficient (b) close to the steady-state Nickel/MacCready value. V_x has only a slight relative maximum (d) and the altitude trace really looks like a dolphin-trajectory (c). The payoff functions Φ (f) are the same at the beginning and the end; they deviate in the upwind region in the typical way discussed above.

The influence of several different windfield types and different airplane parameters is discussed in [5], [6]. Also

analytical approximate solutions for very large and very small windfield lengths are given there. Simulation results show that pilots can fly these trajectories provided the upwind field as well as the optimal trajectory are known to them in advance which usually is not the case. The lastmentioned deficiency may be overcome, at least in an approximate manner, by the use of microcomputers, while knowing the wind field may be out of range.

Literature

- [1] Nickel, K.: Die günstigste Geschwindigkeit des Streckensegelfluges. Aero Revue, Heft 6, S. 223-225, Zürich 1949.
- [2] MacCready, P.: Optimum Airspeed Selector. Soaring, Santa Monica, USA, 1954, H 3/4, p. 8-9.
- [3] Pierson, B.L.; de Jong, J.L.: Cross-country sailplane flight as a dynamic optimization problem. Inst. J. Num. Math. Eng., Vol. 12, pp. 1743-1759 (1978).
- [4] de Jong, J.L.: Instationary Dolphin flight: The optimal Energy Exchange Between a Sailplane and Vertical Currents in the Atmosphere. 2nd IFAC Workshop on Control Appl. of Nonlinear Programming and Optimization. Oberpfaffenhofen, Sept. 15-17, 1980.
- [5] Dickmanns, E.D.: Zeitoptimaler dynamischer Streckensegelflug. erscheint in der ZFW (2 Teile), (1983).
- [6] Dickmanns, E.D.: Optimal periodischer Delphin-Segelflug. Mitteilung aus dem Forschungsschwerpunkt Simulation und Optimierung dynamischer Systeme, LRT, HSBw München, Febr. 1982.

Zusammenfassung

Es wird ein simulierter Datensatz optimaler Durchflüge eines Segelflugzeuges LS 3 (15-m-FAI-Klasse) im Geradeausflug durch ein Aufwindfeld verschiedener Ausdehnung vorgestellt. Dabei ergeben sich 2 Typen von Trajektorien, die an bestimmten Stellen des Aufwindes optimal zu sein scheinen. Der entscheidende Faktor bei einer optimalen Gesamtflugbahn ist die Phugoid-Wellenlänge bei der entsprechenden Nickel-/MacCready-Geschwindigkeit. Die von der Theorie her optimalen Trajektorien können von Piloten nur schwierig ausgenutzt werden, wenn das Aufwindfeld relativ klein ist. Bei grösseren Aufwindfeldern liegt das vertikale Lastvielfache n_z einer optimalen Flugbahn bei etwa 1.